Journal of Thermal Analysis, Vol. 47 (1996) 857-869

THE SYNTHESIS OF MANGANESE–ZINC FERRITE THROUGH THE TRANSFORMATION OF POLYNUCLEAR COORDINATION COMPOUNDS

*Oana Carp**[1], *E. Segal***, *Maria Brezeanu****, *Luminita Patron**, *R. Barjega***** *and N. Stanica***

*Institute of Physical Chemistry 'I. G. Murgulescu' of the Romanian Academy, Splaiul Independentei, Nr. 202, sector 6, Bucharest
**Department of Physical Chemistry, Faculty of Chemistry, University Bucharest, Bulevardul Carol I, Nr. 13, Bucharest
***Department of Inorganic Chemistry, Faculty of Chemistry, University of Bucharest, Dumbrava Rosie Street, Nr. 23, sector 2, Bucharest
****ZECASIN S. A., Chemical Research & Development & Production, Splaiul Independentei, Nr. 202, sector 6, Bucharest, Romania

(Received December 24, 1995)

Abstract

The authors analyse the possibility of obtaining manganese–zinc ferrite through the transformations of polynuclear coordination compounds (pcc), either in the solid state or in a reaction medium. Polynuclear coordination compound precursors with the general molecular formula:

$$[Fe(II)_xFe(III)_y(Mn_{0.5}Zn_{0.5})(C_2O_4)_2(OH)_{y+2}(H_2O)_2]$$

with $0.2<x<1.0$, $1.0<y<1.8$ and $x+y=2$, obtained through a forced hydrolysis were characterized by chemical and physicochemical procedures. A non-isothermal kinetic analysis of the thermal decomposition steps showed that all of them are described by contracting geometry rate equation. The influence of the thermal treatment on the properties of the final products of transformation was evidenced.

Keywords: manganese–zinc ferrite, polynuclear coordination compounds

Introduction

Polynuclear coordination compounds with two or more metallic ions are capable of forming mixed oxides through their thermal decomposition. The syn-

---

[1] Author to whom all correspondence should be addressed.

0368–4466/96/ $ 5.00

John Wiley & Sons, Limited
Chichester

thesis of these oxides using polynuclear compounds as precursors can be performed either in solid state (dry methods) or in a reaction medium (wet methods). A general picture of such transformations for polynuclear coordination compounds is given in the following sequence:

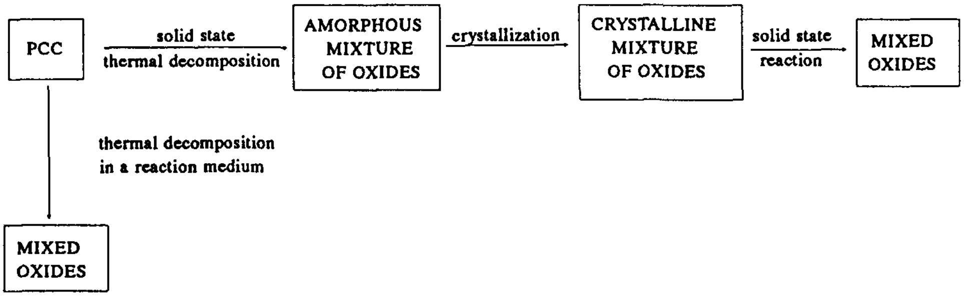

Following our research concerning the synthesis of mixed oxides with high reproducibility and good homogeneity [1–4] this paper presents the preparation of manganese–zinc ferrite through thermal decomposition of polynuclear coordination compounds.

Experimental

As precursors of manganese–zinc ferrite, polynuclear coordination compounds synthesized by forced hydrolysis were used. Ferrous oxalate, manganese acetate or manganese dioxide, and zinc acetate or zinc oxide were used as starting materials.

The compositions of the coordination compounds and the final decomposition products were determined by quantitative analysis: the metal content by atomic adsorption technique, and the carbon and hydrogen contents by means of the usual combustion method.

Data about the stereochemistry of the metal ions were obtained from the electronic spectra at room temperature, recorded with Specord M 40 spectrophotometer, in the range 11.000–54.000 cm^{-1}.

In order to obtain information about the oxalate anions, the IR spectra of the polynuclear compounds were obtained by using the KBr disc technique in the range 200–4000 cm^{-1} with a Specord M-80 type infrared spectrophotometer.

The crystalline states of the compounds used and of the solid decompositions products were investigated by using a Dron 3 X-ray diffractometer with CoK_{α} radiation.

The thermal decomposition curves were obtained with a Q-1500 D Paulik-Paulik-Erdey derivatograph in a static air atmosphere at heating rates in the range 0.6–10 K min^{-1} with α-Al_2O_3 as the inert compound.

The evolved gaseous products were analysed by means of a Hewlett-Packard GC-MS mass spectrometer.

In order to determine the magnetic susceptibility and the saturation magnetization at room temperature, a Faraday balance with $HgCo(SCN)_4$ as calibrant was used.

The values of non isothermal kinetic parameters were obtained by processing thermogravimetric data using two programs, DISCRIM 1 [5] and DISCRIM 2 [6]. Both programs permit selection of the probable mechanism.

Taking into account the possibility of changes in the reaction mechanism with conversion, besides the kinetic analysis of the whole (α, T) curve, the ranges of conversion $0<\alpha<\alpha_{ip}$ and $\alpha_{ip}<\alpha<1$ (the subscript ip means the inflexion point), were analysed, too.

The induction period, when clearly exhibited, was kinetically analysed together with the acceleratory period.

Results and discussion

Characterization of coordination compounds

Depending on the experimental conditions and on the nature of the starting materials, the polynuclear compounds obtained are characterized by the molecular formula

$$[Fe(II)_xFe(III)_y(Mn_{0.5}Zn_{0.5})(C_2O_4)_2(OH)_{y+2}(H_2O)_2]$$

with $0.2<x<1.0$, $1.0<y<1.8$ and the conditions $x+y=2$.

The polynuclear coordination compound with the highest Fe(III) content was obtained when MnO_2 was used as raw material. This result can be explained by the oxidant character of MnO_2, which can contribute to the transformation of Fe(II) to Fe(III). Details about the synthesis of such combinations have been given elsewhere [7].

It is worth mentioning that all the polynuclear coordination compounds synthesized exhibit very similar physicochemical properties. For this reason our discussion will be limited to the compound with $x=0.8$ and $y=1.2$. Some physicochemical properties of the polynuclear combinations obtained are presented in Tables 1 and 2.

The octahedral environment of the iron ions, Fe(II) d^6 and Fe(III) d^5, and the tetrahedral one of Mn(II) d^5, can be inferred from the location of the maxima in the electronic spectra.

The vibrational spectra of the polynuclear coordination compounds studied are similar to those of $Na_2C_2O_4$ and $FeC_2O_4 \cdot 2H_2O$ [8]. This fact indicates the same function of oxalate anions and the not strongly modified character of C–O linkages. The tetradentate oxalate anions keep their planar structure.

Table 1 Data obtained from electronic and vibration spectra

d–d transition of the metal ions						Vibrational modes of the oxalate anion			
Fe(II)		Fe(III)		Mn(II)		cm^{-1}			
Transition	Absorption maxima/cm^{-1}	Transition	Absorption maxima/cm^{-1}	Transition	Absorption maxima/cm^{-1}	$Na_2C_2O_4$	$FeC_2O_4{\cdot}H_2O$	pcc	Assignation
$5T_{2g} \rightarrow {}^5A_g$	10.500	${}^6A_{1g} \rightarrow {}^4T_{1g}$	11.000	${}^6A_1 \rightarrow {}^4T_4$	20.835		3.340s	3.360s	$\nu(H_2O)$
	11.000	${}^6A_{1g} \rightarrow {}^4T_{2g}$	15.000	${}^6A_1 \rightarrow {}^4T_2$	23.200	1.664*			
		${}^6A_{1g} \rightarrow {}^4E_g$	23.000			1.640vs	1.638vs	1.635	ν_a(O–C–O)
						1.485;1.450*			ν_s(O–C–O)
						1.335s	1.360s	1.360s	
						780sh	825s	820	δ(O–C–O)
						774s			
						520s	500s		δ(O–C–O)

The polynuclear coordination compounds studied exhibit a crystalline structure. The coordination compounds' lattice is with monoclinic lattice which is isomorphous with that of $FeC_2O_4 \cdot 2H_2O$. The mean crystallite size calculated for the most intense line using Sherrer's formula [9] is l=470 Å. The fact that the monoclinic structure of the $FeC_2O_4 \cdot 2H_2O$ used as starting material is preserved in the polynuclear coordination compounds, can be taken as a proof that their formation takes place through the intrusion of Mn(II) and Zn(II) in the ferrous oxalate lattice.

Table 2 X-ray and magnetic data

		X-ray powder diffraction data				Magnetic properties	
Number of line	*hkl*	$FeC_2O_4 \cdot 2H_2O$ ASTM 23-293		pcc		μ_{teor}^{*} (BM)	μ_{exp}^{**} (BM)
		d/Å	I/I_o	d/Å	I/I_o		
1	111 002	4.80	100	4.83	100	7.61	6.97
2	200	4.70	65	4.67	93		
3	202	3.880	25	3.877	7		
4	112	3.629	20	3.615	3		
5	211	3.597	25	3.575	6		
6	211	3.172	4	3.155	1		
7	202	3.004	50	2.982	22		
8	020	2.778	4	2.759	1		
9	213	2.654	30	2.649	7		
10	312	2.634	16	2.628	2.5		
11	121	2.616	25	2.606	3		
12				2.546	4		
13	204	2.396	3	2.398	2.5		
14	402	2.355	3	2.356	3		
15	222	2.258	13	2.253	2.5		
16	411	2.224	3	2.221	1		
17	213	2.190	4	2.178	1		
18	123	2.122	9	2.155	2		
19	321	2.106	8	2.063	13		
20	314	2.047	7	2.035	12		
21	413	2.021	14	2.024	24		
22	123	1.980	3	2.006	17		
23	204	1.949	11	1.939	25		
24	402	1.929	9	1.917	23		
25	323	1.893	15	1.891	21		
26	215	1.847	2	1.856	2		

Table 2 Continued

		X-ray powder diffraction data				Magnetic properties	
Number of line	*hkl*	$FeC_2O_4 \cdot 2H_2O$ ASTM 23-293 d/Å	I/I_0	pcc d/Å	I/I_0	μ_{teor}* (BM)	μ_{exp}** (BM)
27.	512 015	1.816	21				
28.	430	1.795	4	1.808	28		

*μ_{teor} (BM) = $\sqrt{\Sigma(\mu_{M_e})^2}$ where μ_{M_e} represents the value of the magnetic moment of a paramagnetic ion present in the polynuclear compound.

**μ_{exp} (BM) = $\sqrt{\frac{3kT}{N}\chi'_M T} = 2.828\sqrt{\chi'_M T}$ where

$\chi'_M = \chi_g M$

χ_g = represents the magnetic susceptibility corresponding to a gram of substance

M = the molecular weight

T = the absolute temperature

k = Boltzmann's constant

N = Avogadro's number.

Taking into account these experimental data, the most probable formulation for these polynuclear coordination compounds can be given as

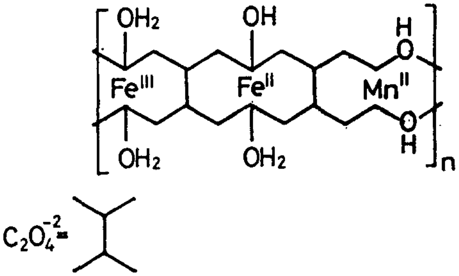

Due to the fact that the ionic radii of the manganese and zinc ions are quite close ($r_{Zn(II)}=0.83$ Å and $r_{Mn(II)}=0.91$ Å after Goldschmith) the Mn(II) ion can be isomorphously substituted by Zn(II) and alternate in the polynuclear chain so that the ratio Fe(II):Fe(III):Zn(II):Mn(II) becomes 1:1:0.5:0.5.

Thermal decomposition of the polynuclear coordination compounds in the solid state

Derivatographic data and mass spectra of the evolved gases indicate that the decomposition of these polynuclear compounds occurs through mixed oxocarbonates. Irrespective of the Fe(III)/Fe(II) ratio, as a consequence of heating, the investigated compounds undergo the following decomposition steps:

$[Fe(II)_xFe(III)_y(Mn_{0.5}Zn_{0.5})(C_2O_4)_2(OH)_{y+2}(H_2O)_3](s) \rightarrow$

$$[Fe(II)_xFe(III)_y(Mn_{0.5}Zn_{0.5})(C_2O_4)_2O_{(y+2)/2}](s) + (4 + y/2)H_2O(s) \qquad (I)$$

$$[Fe(II)_xFe(III)_y(Mn_{0.5}Zn_{0.5})(C_2O_4)_2O_{(y+2)/2}](s) \rightarrow$$

$$[Fe(II)_xFe(III)_y(Mn_{0.5}Zn_{0.5})(CO_3)_2O_{(y+2)/2}](s) + 2CO(g) \qquad (II)$$

$$[Fe(II)_xFe(III)_y(Mn_{0.5}Zn_{0.5})(CO_3)_2O_{(y+2)/2}](s) \rightarrow$$

$$[Fe(II)_xFe(III)_y(Mn_{0.5}Zn_{0.5})CO_3O_{(y+2)/2}](s) + 2CO(g) \qquad (III)$$

$$[Fe(II)_xFe(III)_y(Mn_{0.5}Zn_{0.5})CO_3O_{(y+2)/2}](s) \rightarrow$$

$$Fe_2(Mn_{0.5}Zn_{0.5})O_4(s) + CO_2(g) \qquad (IV)$$

The relatively high temperature of reaction (I) (Table 3) is proof, in addition to the electronic spectrum of the coordination compound, that the evolved water should come from the coordination sphere. This is also in agreement with data published by Logvinenko [10] who mentioned that the water molecules directly bonded to the metal ions are released at a higher temperature.

Table 3 lists the values of the non-isothermal kinetic parameters corresponding to reaction (I) for the entire (α, T) curves and Table 4 lists similar data for its significant portion. In the first case, in which we applied both programs for evaluating the non-isothermal kinetic parameters (DISCRIM 1 and DISCRIM 2), the values obtained are quite close. Indeed the program DISCRIM 2 leads to a value for the reaction order close to 0.66, which corresponds to the contracting sphere mechanism as obtained using the program DISCRIM 1. The relative independence of the non-isothermal kinetic parameters of the heating rates shows no heat-transfer limitation.

Small changes in the values of the activation energy and pre-exponential factor with the heating rate are compensated as shown by the quasi-constancy of $k_{433\ \mathrm{K}}$ values. For the significant portions of the conversion curve ($0<\alpha<\alpha_{ip}$ and $\alpha_{ip}<\alpha<1$) one finds the same kinetic law describing its course. For the first conversion interval, the values of the kinetic parameters are quite close to those obtained for the entire range. For the second one ($\alpha_{ip}<\alpha<1$) slight differences can be observed, probably compensated, in the non-isothermal kinetic parameter values. For the induction period at $\beta=2.5$ K min^{-1}, the most probable kinetic law was found to be $\alpha^n=kt$. The acceleratory period, following the induction period occurs according to the same mechanism and with close values of the non-isothermal kinetic parameters with respect to those corresponding to $0<\alpha<1$ and $0<\alpha<\alpha_{ip}$.

A contracting geometry mechanism was found for the other three reactions investigated (Table 5), with quite comparable probabilities for the contracting sphere and contracting cylinder models.

Table 3 Non-isothermal kinetic parameter values of reaction (I) correspoding to the entrie conversion range

β/ K min^{-1}	T_i – T_f/K	T_{max}/ K	Computation of $f(\alpha)$ program	$f(\alpha)$	A/s^{-1}	E/ kJ mol–1	k(433K)10^2/ s–1	Mean square deviation
10	408 – 493	463	DISCRIM 2	contracting sphere	1.02×10^8	76.2	51.9	3.06
			DISCRIM 1	$(1-\alpha)^n$ n=0.68	5.66×10^8	82.3	53.5	0.15
5	399 – 481	458.5	DISCRIM 2	contracting sphere	6.27×10^8	74.4	61.2	12.65
			DISCRIM 1					
2.5	396 – 468	448	DISCRIM 2	contracting sphere	2.32×10^7	70.5	59.6	11.42
			DISCRIM 1	$(1-\alpha)^n$ n=0.60	1.90×10^7	69.9	58.2	4.92
1.25	394 – 446	435	DISCRIM 2	contracting sphere	8.233×10^8	84.4	53.0	10.56
			DISCRIM 1	$(1-\alpha)^n$ n=0.62	9.23×10^8	85.5	34.4	2.57

T_i = initial temperature of reaction
T_f = final temperature of reaction
T_{max} = temperature of the inflexion point in the TG curve where the reaction attains its maximum rate

Characterization of the final products of thermal decomposition

Chemical analysis of the solid product of reaction (IV) shows that it consists of $Fe_2(Mn_{0.5}Zn_{0.5})O_4$. The diffractograms of the decomposition end products for

Table 4 Non-isothermal kinetic parameter values of reaction (I) corresponding to the significant portion of the α–T curve (DISCRIM 1)

Conversion range	β/K min^{-1}	T_i – T_f/K	$f(\alpha)$	A/s^{-1}	E/kJ mol^{-1}	Mean square deviation
0–α_{ip}						
0–0.5253	10	408 – 463	contracting sphere	4.00×10^8	80.3	0.37
0–0.6570	5	399 – 458.5	contracting sphere	4.68×10^7	72.7	4.90
0–0.6569	2.5	396 – 448	contracting sphere	3.21×10^7	70.7	3.42
0–0.5966	1.25	394 – 435	contracting sphere	8.38×10^8	74.3	3.52
α_{ip}^{-1}						
0.5253–1	10	463 – 493	contracting sphere	2.06×10^7	68.8	2.55
0.6570–1	5	458.5 – 481	contracting sphere	1.90×10^7	68.6	12.74
0.6569–1	2.5	408 – 468	contracting sphere	2.20×10^7	61.8	2.73
0.5966–1	1.25	435 – 447.5	contracting sphere	3.52×10^7	64.7	8.63
induction period						
0–0.2017	2.5	396 –	power law $1/n\times\alpha^{n-1}$ $n = 3/2$	1.41×10^7	71.6	1.52

Table 4 Continued

Conversion range	β/K min^{-1}	T_i – T_f/K	$f(\alpha)$	A/s^{-1}	E/kJ mol^{-1}	Mean square deviation
accelerator period						
0.2017		149	contracting sphere	3.16×10^8	79.1	7.23
	2.5	–				
0.6569		448				

various conditions of calcination shows the existence of the simple oxides (ZnO, MnO and Fe_3O_4), simple ferrites (Fe_2ZnO_4 and Fe_2MnO_4) and double ferrite $Fe_2Mn_{0.5}Zn_{0.5}O_4$. The coupling of these results with the magnetic data obtained suggests a change from the amorphous state to a crystalline one, with a major spinel component, responsible for the appearance of ferromagnetism (Table 6).

Wet method of ferritization

The $Fe_2Mn_{0.5}Zn_{0.5}O_4$ ferrites were obtained as final product of the hydrolytic decomposition of the ferrous oxalate–manganese acetate–zinc acetate system, after 10 h of boiling in an alkaline reaction medium.

The final products, after drying in air are magnetic powders of red–brown colour, which correspond, from the chemical point of view, to the zinc–manganese ferrite:

$$Fe_2Mn_{0.5}Zn_{0.5}O_4\cdot xH_2O \quad \text{with } x=2\text{–}3$$

Spinel phase formation in the product of hydrolysis was confirmed by X-ray and magnetic measurements. One has to emphasize the absence of diffraction lines characteristic of impurities which could be formed in the system (ZnO, MnO, α-FeOOH or α-Fe_2O_3) in the reaction products.

X-ray diffraction data obtained for uncalcined and calcined products evidence the presence of a cubic phase. Table 7 presents the interplanar distances and the corresponding Miller indices for one of these compounds. Due to the overlapping of the diffraction lines, it was impossible to separate the ferrite (or ferrites) from the magnetite compound based on the X-ray data.

The variation (Table 8) of:

- the spinel phase content
- the elementary cell
- magnetic properties

with calcination temperature can be understood by assuming the following mechanism.

Thermal treatment at 200°C (1 h) is accompanied by the transformation of cubic ferrite in the uncalcined compound to a product in which the major component is magnetite. The lattice constant calculated for this product is very close to that of magnetite ($a_{o\ \mathrm{magnetite}}=8.396$ Å, ASTM 19–623).

Table 5 Non-isothermal kinetic parameter values of reaction (II, III and IV), $\beta = 2.5$ K min^{-1}, $0<\alpha<1$

Reaction	T_i – T_f/K	T_{max}/K	Computation of $f(\alpha)$ program	$f(\alpha)$	A/s^{-1}	E/kJ mol^{-1}	Mean square deviation
(II)	486 – 529	503.5	DISCRIM 2	contracting cylinder	1.52×10^{8}	88.8	13.57
				contracting sphere	1.14×10^{11}	116.9	16.62
			DISCRIM 1	$(1-\alpha)^n$ $n=0.53$	9.00×10^{8}	84.8	4.44
(III)	529 – 555	552	DISCRIM 2	contracting cylinder	4.01×10^{7}	91.7	0.32
				contracting sphere	1.25×10^{7}	95.4	0.78
			DISCRIM 1	$(1-\alpha)^n$ $n=0.64$	2.07×10^{7}	90.8	0.26
(IV)	555 – 591		DISCRIM 2	contracting sphere	1.40×10^{10}	121.8	1.48
				contracting cylinder	2.16×10^{7}	87.7	2.55
			DISCRIM 1	$(1-\alpha)^n$ $n=0.71$	1.25×10^{9}	129.6	0.87

Table 6 Data concerning the residual decomposition products obtained through solid-state thermal decomposition of the pcc

Thermal treatment	Fe_3O_4 (content)*	Ferrite** (content)	a*** Å	μ_{exp} (BM)
Calcination 1h–400°C slow cooling	1	1	8.438	0.35
Calcination 1h–450°C 1h–400°C slow cooling	1.9	1.3	8.458	1.79

* The content is calculated by comparing the 100% relative intesities to the lowest values of these.

** In this term are included the simple ferrites (Fe_2ZnO_4 and Fe_2MnO_4) and the double one $Fe_2(Mn_{0.5}Zn_{0.5})O_4$

*** The elementary cell calculation was preformed as if there were only a single phase in the residual decomposition product.

Table 7 X-ray diffraction data for the manganese–zinc ferrite obtained by the wet method

hkl	Uncalcined compound		Calcined compound 1h–200°C slow cooling		Calcined compound 1h–200°C 1h–400°C slow cooling	
	d/Å	I/I_0	*d*/Å	I/I_0	*d*/Å	I/I_0
220	2.966	35.5	2.960	40	2.958	41
311	2.535	100	2.523	100	2.529	100
400	2.098	20	2.092	26	2.091	26
422	1.714	12	1.713	15		
511	1.616	23	1.611	26	1.614	21
440	1.485	31.5	1.481	33.5	1.482	33

Table 8 Structural and magnetic properties of the manganese–zinc ferrite obtained by the wet method

Thermal treatment	Lattice constant Å	Magnetization of saturation σ_s (emu/g)	Spinel phase content I/I_0
Uncalcined compound	8.466	3.69	1.26
Calcination 1h–200°C slow cooling	8.405	51.43	1
Calcination 1h–400°C 1h–200°C slow cooling	8.405	33.85	1.11

Further thermal treatment at 400°C (1 h) leads to retransformation of magnetite to ferrite. A product with a lattice constant close to the uncalcined compound and mixed ferrite is obtained ($a_{o(Zn,\ Mn,\ Fe)(Fe,\ Mn)O_4}$=8.474 Å. ASTM 10–467).

References

1 M. Brezeanu, L. Patron, O. Carp, A. Antoniu, M. Andruh and A. Gheorghe, Rev. Roum. Chim., 38 (1993) 1291.

2 O. Carp, E. Segal, L. Patron, R. Barjega, C. Craiu and N. Stanica, Thermochim. Acta, 228 (1993) 249.

3 O. Carp, E. Segal, L. Patron, R. Barjega and N. Stanica, Thermochim. Acta (in press).

4 O. Carp and E. Segal, Rev. Roum. Chim. (in press).

5 T. Coseac and E. Segal, Thermochim. Acta, 149 (1991) 189.

6 O. Carp and E. Segal, Thermochim. Acta, 185 (1991) 111.

7 M. Brezeanu, L. Patron, E. Cristurean, D. Marinescu, A. Antoniu, M. Andruh, O. Carp, N. Stanica and A. Gheorghe, Rev. Roum. Chim. 38 (1993) 1173.

8 K. L. Scott, K. Weighart and A. K. Skyles, Inorg. Chem., 12 (1973) 655.

9 H. Klug, L. E. Alexander, (Eds) 'X-ray Diffraction Procedure' J. Wiley & Sons, New York 1962, p. 461.

10 V. A. Logvinenko, L. I. Myachina and G. V. Gavrilova, J. Thermal Anal., 29 (1984) 1095.